Drug Design, Development and Therapy

Dovepress
open access to scientific and medical research

Open Access Full Text Article

ORIGINAL RESEARCH

A Novel Nanomicellar Combination of Fenretinide and Lenalidomide Shows Marked Antitumor Activity in a Neuroblastoma Xenograft Model

This article was published in the following Dove Press journal:
Drug Design, Development and Therapy

Isabella Orienti[1]
Ferro Nguyen[2]
Peng Guan[2]
Venkatadri Kolla[2]
Natalia Calonghi[1]
Giovanna Farruggia[1]
Michael Chorny[2]
Garrett M Brodeur[2]

[1]Department of Pharmacy and Biotechnology, University of Bologna, Bologna 40127, Italy; [2]Divisions of Oncology, Children's Hospital of Philadelphia, Philadelphia, PA 19104, USA

Purpose: Currently >50% of high-risk neuroblastoma (NB) patients, despite intensive therapy and initial partial or complete response, develop recurrent NB due to the persistence of minimal residual disease (MRD) that is resistant to conventional antitumor drugs. Indeed, their low therapeutic index prevents drug-dose escalation and protracted administration schedules, as would be required for MRD treatment. Thus, more effective and less toxic therapies are urgently needed for the management of MRD. To address this aim, we evaluated a new combination of fenretinide and lenalidomide, both endowed with antitumor activity and low-toxicity profiles. New nanomicelles were prepared as carriers for this combination to maximize bioavailability and accumulation at the tumor site because of the enhanced permeability and retention (EPR) effect.

Experimental design: New nanomicelles containing the fenretinide–lenalidomide combination (FLnMs) were prepared by a one-step method, providing high drug encapsulation and micelle dimensions suitable for tumor accumulation. Their administration to mice bearing human NB xenografts allowed us to evaluate their efficacy in comparison with the nanomicelles containing fenretinide alone (FnMs).

Results: Treatment by FLnMs significantly decreased the tumor growth of NB xenografts. FLnMs were more active than FnMs despite comparable fenretinide concentrations in tumors, and lenalidomide alone did not show cytotoxic activity in vitro against NB cells. The tumor mass at the end of treatment with FLnMs was predominantly necrotic, with a decreased Ki-67 proliferation index.

Conclusion: FLnMs provided superior antitumor efficacy in NB xenografts compared to FnMs. The enhanced efficacy of the combination was likely due to the antiangiogenic effect of lenalidomide added to the cytotoxic effect of fenretinide. This new nanomicellar combination is characterized by a low-toxicity profile and offers a novel therapeutic option for the treatment of high-risk tumors where the persistence of MRD requires repeated administrations of therapeutic agents over long periods of time to avoid recurrent disease.

Keywords: neuroblastoma, drugs combination, nanomicelles, fenretinide, lenalidomide

Introduction

Most therapeutic protocols for childhood cancers use cytotoxic agents that have a low therapeutic index and result in significant short- and long-term toxicities. This prevents further drug dose-escalation and limits the long-term treatment that is necessary for the complete eradication of the malignant disease. The persistence of drug-resistant MRD after cytotoxic chemotherapy is a frequent cause of relapse and treatment failure.[1] In high-risk neuroblastoma (NB), despite intensive therapy, more than 50% of patients develop the recurrent disease due to the persistence of MRD that is unresponsive to

Correspondence: Isabella Orienti
Email isabella.orienti@unibo.it

submit your manuscript | www.dovepress.com
DovePress
http://doi.org/10.2147/DDDT.S221909

conventional antitumor drugs.[2] Therefore, new antitumor treatments with low toxicity are urgently needed for high-risk cancers such as NB. Many approaches are currently being developed, including immunotherapy, gene therapy, synergistic combinations and repurposing therapy.[3] Another approach is the enhanced drug delivery to solid tumors using nanoparticles as carriers of active agents. Indeed, nanoparticles selectively accumulate in solid tumors based on their size, which allows extravasation through the leaky tumor vasculature that characterizes rapidly growing tumors. The selective accumulation increases the drug concentration in the tumor microenvironment, thus improving its pharmacological efficacy, while at the same time reducing the toxicity associated with conventionally administered antitumor drugs.

The use of nanoparticles as carriers for alternative, antitumor bioactive molecules (AABMs), is an emerging trend in bio-nanomedicine aimed at administering tolerable combinations of antitumor agents for long periods of time (months or years) until complete tumor eradication is achieved. AABMs may be of natural origin (e.g., berberine, curcumin, resveratrol, etc.) or vitamin analogues, such as fenretinide (N-4-hydroxyphenyl-retinamide) or 13-cis-retinoic acid.[4] They are characterized by high tolerability, and their antitumor effect mechanisms do not induce multidrug resistance. However, their hydrophobic character strongly limits their bioavailability, and their low pharmacological potency only provides antitumor activity at high concentrations that are difficult to achieve in vivo using conventional formulations. We hypothesized that the use of nanoparticles as carriers for these molecules would increase their concentrations at the tumor site to levels sufficient to have significant antitumor activity. Moreover, the combination of AABMs with antiangiogenic drugs might further improve their antitumor effect.

In this study, we used the AABM fenretinide in combination with the antiangiogenic drug lenalidomide in novel nanomicelles designed to provide high encapsulation efficiency and drug loading capacity. We evaluated their antitumor activity in an NB xenograft model.

Fenretinide is a semi-synthetic retinoid characterized by high cytotoxic efficacy against a wide range of cancer cells in vitro and previously investigated as a potential anticancer and chemopreventive drug.[5–13] Among the AABMs, fenretinide has a superior pharmacological profile due to its ability to induce cytotoxicity by multiple mechanisms[14–18] and to target cancer stem cell-associated molecular targets.[19–22]

Previous clinical Phase I–III evaluations of fenretinide showed minimal systemic toxicity and good tolerability.[9,23,24] However, clinical trials aimed at evaluating the activity of fenretinide in cancer patients yielded disappointing results, likely due to the low bioavailability of the initial oral capsule formulation.[5,10,23–25]

Many attempts have been subsequently made to increase fenretinide bioavailability, including drug incorporation in a lipid solid matrix or in a lipid emulsion. These approaches provided improved performance compared to the initial capsule formulation. However, they still faced problems probably related to the strong drug-lipid association that limited drug release, requiring high drug doses to achieve therapeutic plasma drug concentrations.[26–29]

The recent approach of fenretinide nanoencapsulation in amphiphilic macromolecules, polymers or phospholipids, provided high levels of aqueous drug solubilization, bioavailability and absorption at the tumor site.[30–38] Preclinical studies on nanoformulations of fenretinide-cyclodextrin complex[37] and fenretinide-phospholipid salts[38] indicated high antitumour activity in cancer stem cells of various origins in vitro, and in tumour xenografts derived from cancer stem cells of lung cancer, colon cancer and melanoma origin. Moreover, higher drug concentrations in blood and tumours were obtained in the absence of toxicity.

Therefore, fenretinide nanoencapsulation in combination with other drugs that have antitumor activity and low toxicity may represent a further step towards the realization of new therapeutic systems able to elicit effective therapeutic responses in vivo, avoiding the need of conventional antitumor drugs and their related short- and long-term toxicities.

Lenalidomide was selected to combine with fenretinide because of its antiangiogenic properties and its acceptable toxicity profile that has made it the standard drug used for long-term treatment of multiple myeloma and other cancers.[39–43] The anti-angiogenic effect of lenalidomide has not been fully evaluated in NB so far. However, lenalidomide was reported to overcome the suppression of natural killer cells in NB microenvironment, by activation of T cells to secrete IL-2.[44] Therefore, this drug might be particularly interesting in NB tumors, which are characterized by high vascularization[45] and immune suppressive activity as well as in other highly vascularized, tumor types.

Materials and Methods

Chemicals

Fenretinide (N-4-hydroxyphenyl-retinamide, 4-HPR) was purchased from Olon Spa (Milan Italy), Lenalidomide from AstaTech Inc (PA, USA) Soy L-α-phosphatidylcholine,

glyceryl tributyrate, hydroxypropyl-beta-cyclodextrin (Mw 1460) and KOH from Sigma-Aldrich. Ethanol absolute anhydrous was purchased from Carlo Erba Reagents.

Nanomicelles Preparation

Soy phosphatidylcholine (4 mmoles), glyceryl tributyrate (2 mmoles) and KOH 10 N (4 mmoles) were mixed with hydroxypropyl-beta-cyclodextrin (0.8 mmoles) to obtain a semisolid phase. Fenretinide (1 mmole) was dissolved in ethanol (300 µL) and KOH 10 N (1 mmole) and was subsequently added to the mixture. Homogenization was carried out in a mortar grinder (RM 200 Retsch Verder Italy) for 30 mins at 100 min^{-1} rate. Afterwards, lenalidomide (0.5 mmoles) was added, and mixing was continued for another 30 mins until homogeneity. The resultant semisolid phase was dissolved in water (50 mg/mL) at 37 °C. The liquid dispersion obtained was purified by size exclusion chromatography (SEC), using PD-10 columns packed with Sephadex G-25 medium (GE Healthcare Life Sciences) and hydrated with water.[46] A subsequent filtration through 0.4 µm and 0.2 µm cellulose acetate filters (Fisher Scientific) yielded the final dispersion of the fenretinide–lenalidomide-loaded nanomicelles (FLnMs) suitable for in-vivo use. Nanomicelles without drugs (nMs) or containing fenretinide alone (FnMs) were prepared by the same procedure.

Differential Scanning Calorimetry (DSC)

Thermograms of pure drugs and semisolid mixtures containing the drugs were carried out using Mettler equipment (Greifensee, Switzerland: FP 80HT control unit, FP 85TA cell furnace, and FP 89 control software). Samples of about 10 mg were weighed and analyzed in the range of 20−250 °C, at a heating rate of 10 °C min^{-1}.

Drug Content in the Nanomicelles

In order to evaluate their drug content, the nanomicelle dispersions were diluted (1:3 v:v) with an ethanol:water (1:1, v:v) mixture and analyzed by UV spectroscopy (Shimadzu UV-1601) at 360 nm for fenretinide and 250 nm for lenalidomide, in comparison with the empty nanomicelles. The concentrations obtained represented the drugs encapsulated in the nanomicelles and free in the aqueous phase. Therefore, to obtain the concentrations of free drugs, the nanomicelle dispersions were centrifuged in a 3.5 mL Ultra 5 KDa filter (Merck Millipore) at 4000 x g for 30 min, and the ultrafiltrate was spectrophotometrically analyzed for drug content, after dilution 1:3 with an ethanol:water (1:1, v:v) mixture. The difference between the whole drug concentration in the nanomicelle suspension and in the ultrafiltrate provided the concentration of the encapsulated drugs. The drug loading was obtained as the ratio between the concentration (w:v) of the encapsulated drug and the concentration (w:v) of the nanomicelle dispersion. The encapsulation efficiency as the ratio between the concentration (w:v) of the encapsulated drug and the whole drug concentration (w:v) obtained by spectrophotometric evaluation of the liquid dispersion before purification by SEC.

Stability of the Nanomicelles Towards Drug Leakage

The stability of the nanomicelles was measured by dialysis at 37 °C. The nanomicelle dispersions were diluted 1:10 (v:v) with PBS (pH 7.4) containing 25% human plasma and placed in a dialysis bag (Mw cutoff 5KD) (Fisher Scientific) immersed in a receiving compartment containing PBS (pH 7.4) and n-octanol 5% (v:v). N-octanol was added to serve as a drug-extractive phase simulating the presence of cell membranes in vivo.[47] Spectrophotometric analysis in the releasing phase was made at increasing time intervals, as described above.

Dynamic Light Scattering (DLS) Characterization

Particle size, polydispersity and zeta potential were measured at 37 °C on the nanomicelle dispersions diluted 1:10 with water (Malvern Instruments, Worcestershire, UK). A minimum of 12 measurements per sample were made. Results were the combination of three 10 min runs for a total accumulation correlation function time of 30 mins. The results were volume-weighted.

Confocal Laser-Scanning Fluorescence Microscopy (CLSFM)

Specimens were analyzed using a Nikon C1s confocal laser-scanning microscope, equipped with a Nikon PlanApo 60, 1.4-NA oil immersion lens. Excitation light for fenretinide was obtained by an Argon Ion Laser (405 nm), and emission was recorded at 650 nm. Optical sections were obtained at increments of 0.01 µm in the Z-axis and were digitized with a scanning mode format of 512–512 pixels. Image processing was performed using ImageJ software.

Cell Lines

SH-SY5Y NB cells stably transfected with NTRK2 (clone BR6)[48] were used for the in-vitro experiments. We tested

the integrity and authenticity of these cell lines for endotoxins, mycoplasma, bacterial and other viral contaminations, and we tested the genetic authenticity of this line by multiplex PCR techniques. These tests were performed on an annual basis at the cell center services facility of the University of Pennsylvania. Cells were grown in RPMI-1640 medium (Gibco) containing 10% fetal bovine serum (Cellgro) and maintained in 150 cm^3 culture flasks (Corning) in a humidified atmosphere of 95% air and 5% CO_2. Transfected cells were maintained in media containing 0.3 mg/mL G418 sulfate (stock solution: 20 mg/mL; Corning). Cells were harvested using 0.02% tetrasodium EDTA in phosphate-buffered saline (PBS).

In vitro Experiments

The in vitro effect of FLnMs was evaluated in comparison with FnMs. We plated 8 x 10^3 cells per well in 96-well plates and exposed the cells at FLnM and FnM concentrations corresponding to 10, 20, 30 μM fenretinide. The free drugs were also tested at concentrations comparable with those contained in the nanomicelles. In this case, fenretinide and lenalidomide were dissolved in ethanol at 1 mM and diluted with cell medium to the final experimental concentrations. Viability was evaluated over time using the Incucyte live cell imaging system (Essen BioScience, MI, USA) and the image analysis software (S3 Base Software).

Mice

We obtained six-week-old female athymic nude mice from Jackson Laboratories. Mice were maintained under humidity- and temperature-controlled conditions in a light/dark cycle that was set at 12 hr intervals. The Institutional Animal Care and Use Committee (IACUC) of the CHOP Research Institute approved the mouse xenograft studies described in this report. The studies were conducted in accordance with all international, USDA, PHS, AAALAC, state, and local rules, regulations and ethical principles regarding the use of animal subjects in research.

Flank Xenograft Experiments

Female athymic nude mice were injected subcutaneously in the right flank with 1 x 10^7 TrkB-expressing SY5Y (BR6) cells suspended in 0.1 mL of Matrigel (Corning, Tewksbury, MA). Tumors were measured manually 2x/week in 2 dimensions (mm) using a caliper. The volume (cm^3) was calculated as follows: [(0.523 x L x W2)/1000)] where L > W. Body weights were obtained 2x/week, and treatment doses adjusted if there was a >10% change in body weight. When tumors reached a mean volume of 0.1 cm^3, the mice were treated with FLnMs or FnMs by IV route 3 times/week for 3 weeks at the dose of 30 mg/kg fenretinide and 17 mg/kg lenalidomide.

Histological Evaluation of Tumors

End point tumors were excised, fixed in 4% paraformaldehyde and delivered to the CHOP Pathology Core for processing and histochemical staining. Stains used included hematoxylin and eosin (H&E), and Ki-67 to assess proliferation.

Evaluation of Fenretinide in Mouse Blood and Tumors

The concentration of fenretinide was evaluated in blood and tumors after intravenous administration of FLnMs or FnMs either as a single administration or as a chronic administration 3 times/week for 3 weeks. After single administration, blood and tumor were collected at 4, 24 and 48 hrs after treatment. For chronic administration, blood and tumor were collected at 24 hrs after the last treatment. Blood was obtained via retro-orbital and terminal bleeds and collected into 2 mL tubes containing sodium heparin (Becton Dickinson). Tumors were collected after sacrifice. Plasma was separated from the blood by centrifugation for 15 mins at 2000 × g at 4°C and stored separately. All samples were stored in −80°C until analyzed by the CHOP Pharmacology Core. Total fenretinide levels were analyzed in mouse plasma and tumor homogenates by UPLC-MS/MS. Tumors were homogenized using a Biologics Inc. Model 3000 ultrasonic homogenizer. We added 20:80 methanol: water with 1% formic acid to a known weight of tissue to obtain a ratio of 4 mL/g sample. Samples were homogenized on ice and frozen until analysis. Standards were prepared in CD-1 mouse plasma containing sodium heparin as an anticoagulant. A nine-point calibration curve was prepared at different concentrations by spiking a working stock. Plasma and tumors homogenate samples were extracted via acetonitrile precipitation in a 96-well format. Electrospray ionization in the negative ion mode was utilized for the tandem mass spectrometric detection of fenretinide (m/z 391.55→ and m/z 391.55→) using AB Sciex 4000 mass spectrometer. Separation was accomplished utilizing Kinetex PFP (50.4.1 mm id, 2.6 μm) column with Shimadzu LC 20AD HPLC system with a run time of 4.5 mins. This assay was linear over the range of 1 to 1000 ng/mL for both fenretinide and fenretinide in mouse plasma. The matrix factors of the mouse tumor obtained using tissue

homogenates spiked with 100 ng of fenretinide per mL (n = 3) against mouse plasma calibration curves were applied in the drug assay calculations.[48]

Statistical Analysis

All assays were performed at least in triplicate and expressed as mean ± SD. Statistical significance was determined by unpaired Student's *t*-test. The data were analyzed by SPSS 20.0 software. Mouse overall survival was determined using the Kaplan–Meier method. *P* values <0.05 were considered significant.

Results

Characterization of the Nanomicelles

Nanomicelles carrying the fenretinide–lenalidomide combination were prepared by simple dissolution in water of a semisolid phase containing soy phosphatidylcholine, glyceryl tributyrate and hydroxypropyl-beta-cyclodextrin (Figure 1). Confocal laser-scanning fluorescence images, obtained by exploiting the spontaneous autofluorescence of fenretinide, showed spherical drug localization inside FnMs and FLnMs (Figure 2A). Image processing of the optical sections of the nanomicelles indicated that fenretinide was homogeneously distributed in the inner core of both FnMs and FLnMs (Figure 2B).

The thermograms of the semisolid phase containing fenretinide or fenretinide + lenalidomide showed low melting peaks in the range 120–140 °C, much lower than the peaks of the pure drugs and at lower temperatures than the single melting endotherms of the pure drugs (Figure 3). This suggests that the drugs are mostly solubilized rather than physically dispersed in the semisolid phase, and the interactions they establish with the mixture components unsettle their crystalline state toward an amorphous, dispersed state. The mean size of the nanomicelles ranged from a minimum of 137.7 ± 0.8 for FLnMs to a maximum of 256.5 ± 6.1 for nM, in the range for tumor accumulation by the EPR effect. Polydispersity was always lower than 0.3, indicating good dimensional homogeneity. The zeta potential was negative, with values between - 65.45 and −71.35 mV. (Table 1). The encapsulation efficiency was slightly higher for fenretinide than lenalidomide: the drug loading was 7.34 ± 0.4 for fenretinide and 4.25 ± 0.5 for lenalidomide (Table 1).

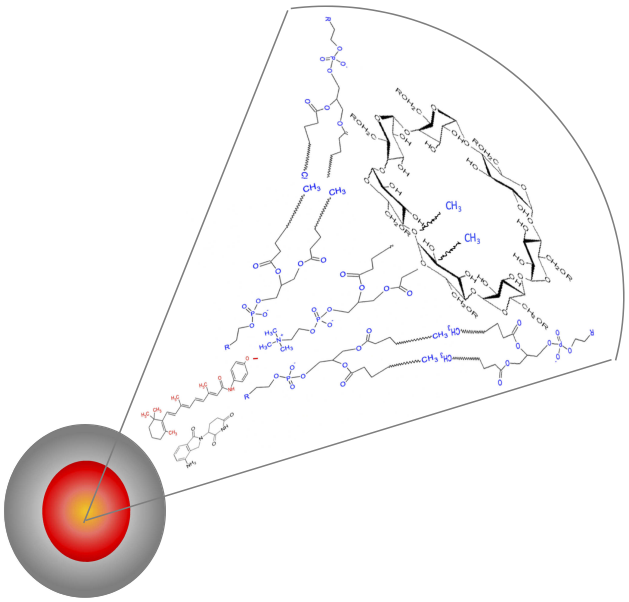

Figure 1 Schematic representation of FLnMs composed of phospholipids and hydroxypropyl-beta-cyclodextrin in the outer layer and fenretinide + lenalidomide in the inner core.

Stability Towards Drug Leakage

The drug leakage from the FLnM micelles was very low: after 48 h, 17% ± 6.2 fenretinide and 23% ± 8.3 lenalidomide were released, indicating nanomicelle stability towards the release of both drugs in time frames longer than the circulation time (Figure 4).

In vitro Cytotoxicity of FLnMs

The cytotoxicity of FLnMs was both time- and dose-dependent (Figure 5A). No significant differences were observed between FLnMs and FnMs, indicating that the presence of lenalidomide did not improve the in vitro cytotoxic activity of fenretinide. Indeed, pure fenretinide provided a cytotoxic effect comparable to FnMs and slightly higher than FLnMs (Figure 5B). Pure lenalidomide was tested at the same concentrations as fenretinide (10 μM, 20 μM, 30 μM) that slightly exceeded the lenalidomide concentration in FLnMs (6.6 μM, 13.2 μM, 19.86 μM) (Figure 5B). However, no cytotoxic effect was observed with pure lenalidomide, consistent with the lack of improved cytotoxicity of FLnMs. Empty nanomicelles, evaluated at the same concentrations as the loaded ones, had no cytotoxic effect over time (all P<0.05).

In vivo Efficacy of FLnMs

In vivo, FLnMs generated a significant antitumor effect, higher than FnMs. (Figure 6A). The tumor growth in FLnM-treated mice was slow and, at the end of administration period, the mean tumor weights (0.12 ± 0.01 g) were much lower than from the FnM-treated mice (0.49 ± 0.03 g) (P <0.05). Also, the

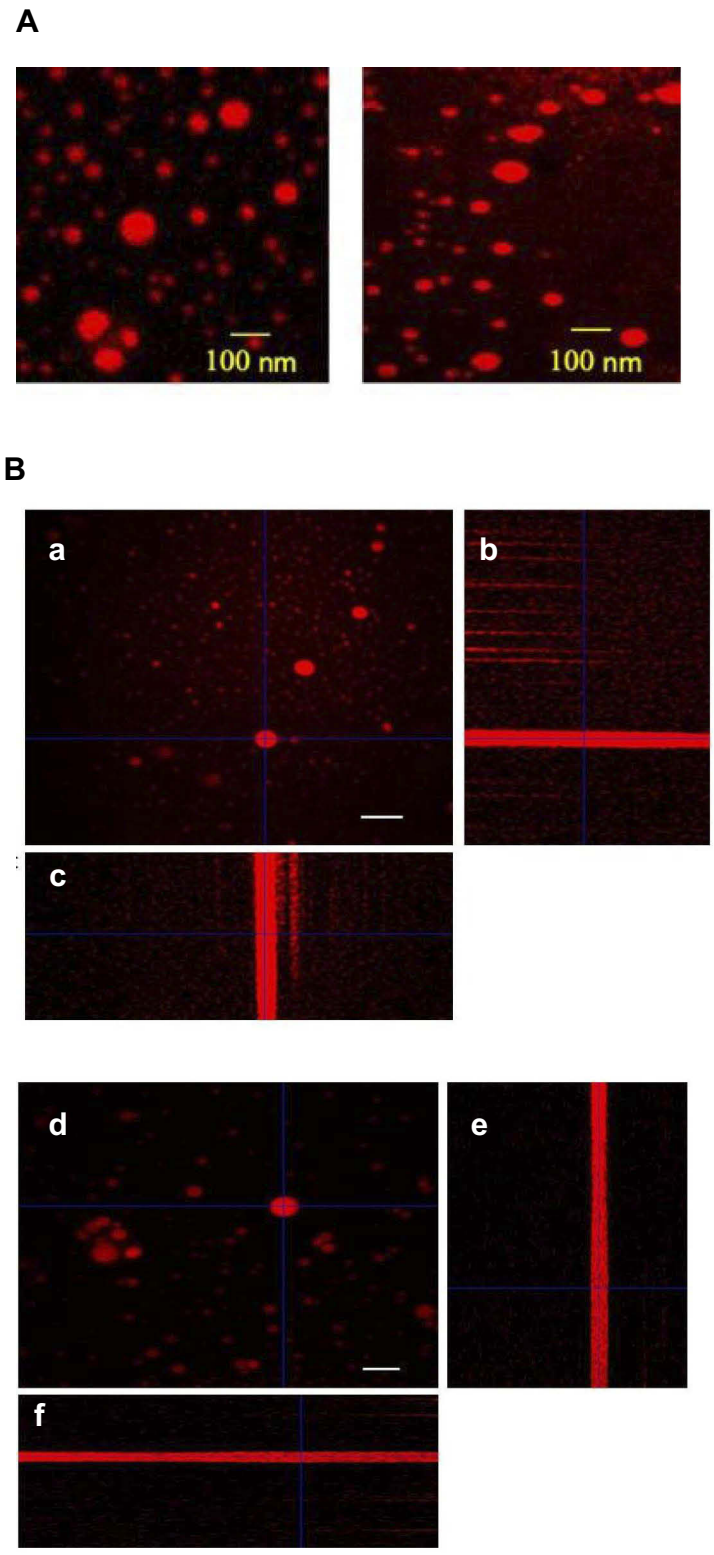

Figure 2 Confocal Laser Scanning image of FLnMs (right) and FnMs (left) showing the presence of autofluorescent fenretinide within micelles (**A**). 2D representation of 125 depth-resolved slices separated by 10 nm (**B**). (a) trans-axial slice (XY plane) through FLnMs: (b) XZ cross-section of planes indicated by horizontal line. (c) YZ cross-sections of planes indicated by vertical line (Bar = 200 nm). (d) trans-axial slice (XY plane) through FnMs: (e) YZ cross-section of planes indicated by vertical line. (f) XZ cross-sections of planes indicated by horizontal line (Bar = 200 nm).

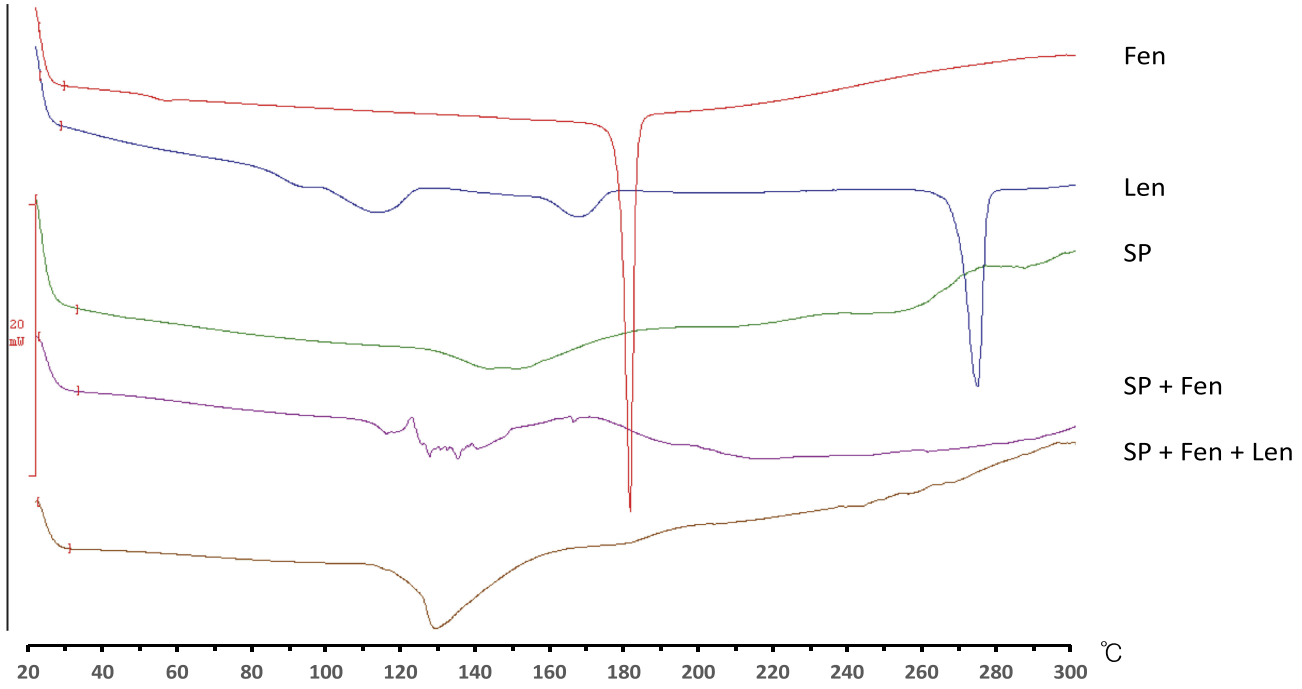

Figure 3 Differential scanning calorimetry of the drugs-semisolid phase mixtures: semisolid phase without drugs (SP), mixture with Fenretinide (SP + Fen), mixture with Fenretinide and Lenalidomide (SP + Fen + Len), pure Fenretinide (Fen), pure Lenalidomide (Len).

survival at the end of treatment was 100% in the FLnM-treated mice compared to 70% in FnM-treated mice (Figure 6B) ($P< 0.05$). The mean body weight of the mice either treated with FLnMs or FnMs increased over time, as in the controls, indicating that neither formulation caused significant systemic side effects (Figure 4C) ($P > 0.05$).

Evaluation of Fenretinide in Mouse Plasma and Tumors

The concentration of fenretinide in plasma and tumor tissue was higher at 4 h than 24 h and 48 h after either FLnM and FnM administration (Figure 7A and B) ($P<0.05$). In tumors, the drug concentrations were always higher than in plasma at each time point from both FLnMs and FnMs (Figure 7B) ($P<0.05$). The drug concentration in tumors was particularly high 4 h after FLnM administration. No significant differences were observed in drug plasma levels either after single and chronic administration of FLnMs and FnMs (Figure 7C). The chronic administration improved fenretinide concentrations in tumors only with FnM administration, whereas there was a slight decrease in tumor drug concentration with chronic vs single FLnM administration (all $P<0.05$).

Histologic Evaluation of Tumors

Untreated tumors appeared undifferentiated, with many compact tumor cells and a high proliferation index (>30%), as demonstrated by Ki-67 index (Figure 8). The tumors treated with FnMs were less compact and had a lower proliferation index (<25%) compared to untreated tumors (all $P<0.05$). Cells were large, differentiated and characterized by a ganglion-like appearance. The tumors treated with FLnMs exhibited a dramatically different appearance both grossly and microscopically. They were

Table 1 Physico-Chemical Characteristics of the Nanomicelles

Micelle Type	Mean Size (nm)	Polydispersity	Zeta Potential (mV)	Encapsulation Efficiency %		Drug Loading % (w:w)	
				Fenretinide	Lenalidomide	Fenretinide	Lenalidomide
nMs	256.5 ± 6.1	0.291 ± 0.017	−65.45 ± 2.1				
FnMs	204.1 ± 2.6	0.258 ± 0.008	−69.17 ± 1.4	91.5 ± 3.2		7.76 ± 0.7	
FLnMs	137.7 ± 0.8	0.258 ± 0.006	−71.35 ± 0.6	89.4 ± 5.0	85.1 ± 1.6	7.34 ± 0.4	4.25 ± 0.5

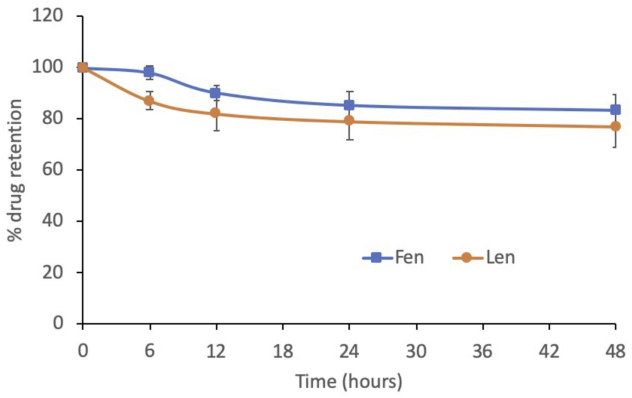

Figure 4 Leakage of fenretinide and lenalidomide from FLnMs in PBS (pH 7.4) containing 25% human plasma at 37° C. All data are the average of at least three different experiments ± SD.

loosely associated with very few viable cells embedded in a discontinuous fibrous network with abundant neuropil, and the proliferation index was very low (<3%) (Figure 8) ($P<0.05$).

Discussion

In this study, we used fenretinide in combination with lenalidomide in novel nanomicelles designed to provide high encapsulation efficiency and drug loading capacity, as well as stability to reduce drug leakage, and a size suitable for tumor extravasation. We prepared the nanomicelles by a new, single-step method, involving a rapid dissolution in water of a semisolid amphiphilic phase consisting of a mixture of lipids, phospholipids, and hydroxypropyl-beta- cyclodextrin, containing the drugs in a solubilization state. The self-aggregation in water of the amphiphilic mixture provided nanomicellar structures with drug localization in their inner cores as revealed by confocal scanning microscopy. The complete solubilization of the drugs in the semisolid phase, as indicated by the DSC thermograms, provided high encapsulation efficiency and stability of the nanomicelles to drug leakage. This was in accordance with the molecular interactions established by the drugs with the mixture components in the semisolid phase that persist in the nanomicellar structures. These characteristics, together with the small size and low dimensional polydispersity, made the nanomicelles suitable for drug accumulation in solid tumors by the EPR effect.

As it is well known, the EPR effect mainly relies on the ability of nanoparticles injected in the bloodstream to accumulate in solid tumors by extravasation through the capillary discontinuities generated by the tumor angiogenesis.[49]

The nanoparticles demonstrate the accumulation of the loaded drugs at extents that depend on both the nanoparticle drug loading and their ability to extravasate. As a result, the EPR effect provides drug accumulation in tumors while limiting drug distribution to other body compartments. Accordingly, this increases the therapeutic efficacy and minimizes the side effects of the administered drugs.[50]

One of the main nanoparticle characteristics that improve their efficiency for drug accumulation in tumors is stability to drug leakage during their circulation time, allowing them to carry more drug to the tumor. Additionally, high drug loading and a mean size under 200–250 nm that facilitates extravasation may further increase the efficiency of drug accumulation.[49,50] The FLnM and FnMs nanomicelles have all these features and are particularly useful to exploit the EPR effect with high efficiency.

Indeed, the intravenous administration of FLnMs and FnMs provided very high fenretinide concentrations in tumors. The concentrations were higher in tumors than in plasma either at 4 h, 24 h and 48 h after administration of both FLnMs and FnMs, indicating an efficient accumulation of the nanomicelles in the NB tumors. Moreover, the lower mean size of the FLnM nanomicelles might account for the higher fenretinide concentration in tumors obtained 4 h after administration (Figure 7A and B).

In particular, the administration of 30 mg/kg fenretinide by FLnMs and FnMs provided 60.8 μg/mL (155.28 μM) and 52.36 μg/mL (133.72 μM) drug concentrations in tumors, respectively, at 4 h. These values are much higher than the concentration range of 1–10 μM that is reported to be active in vitro in a variety of human cancer cell lines, including head and neck cancer, non-small cell lung and small cell lung cancer, breast cancer, ovarian cancer, prostate cancer and pancreatic cancer, as well as neuroblastoma, Ewing's family tumors, leukemia, and multiple myeloma.[29] No data are reported in the literature about fenretinide concentrations in tumors, after intravenous administration of the drug, to compare with FLnMs and FnMs.

A comparison can be made with a nanoformulation of fenretinide recently developed for oral use.[38] In this case, the fenretinide concentrations in tumor xenografts obtained 3 h after administration of 100 mg/kg fenretinide were 3.44 ug/mL (8.78 μM), 1.71 ug/mL (4.36 μM) and 4.98 ug/mL (12.71 μM) in lung cancer, melanoma and colon cancer xenografts, respectively.

In spite of the differences in tumor types, the comparison clearly shows the superiority of intravenous over oral

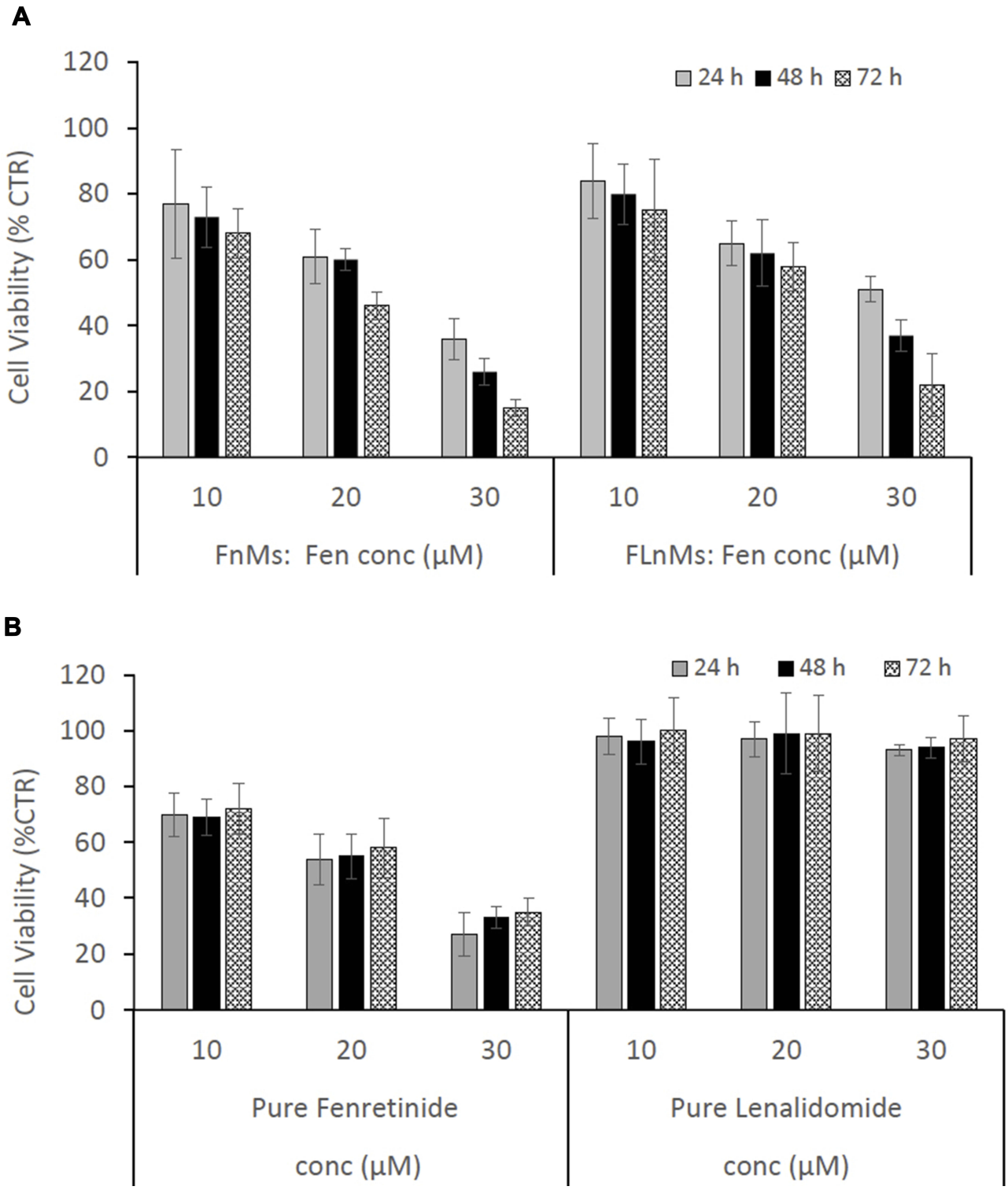

Figure 5 Cytotoxic activity of FnMs and FLnMs at increasing fenretinide concentrations in BR6 cells (**A**). Cytotoxic activity of pure fenretinide and pure lenalidomide at increasing concentrations in BR6 cells (**B**). The cells were exposed at the indicated drug doses and cell viability was evaluated by Incucyte after 24, 48 and 72 hrs and indicated as percentage versus control cells (mean ± SD, n = 8).

administration for the nanoformulated drug. Indeed, the drug concentrations in tumors obtained by the intravenous administration of 30 mg/kg fenretinide were more than tenfold higher than those obtained with 100 mg/kg fenretinide administered by oral route. This is in accordance with the ability of the intravenously injected FLnM and FnM nanoparticles, carrying the loaded drugs, to accumulate in solid tumors.

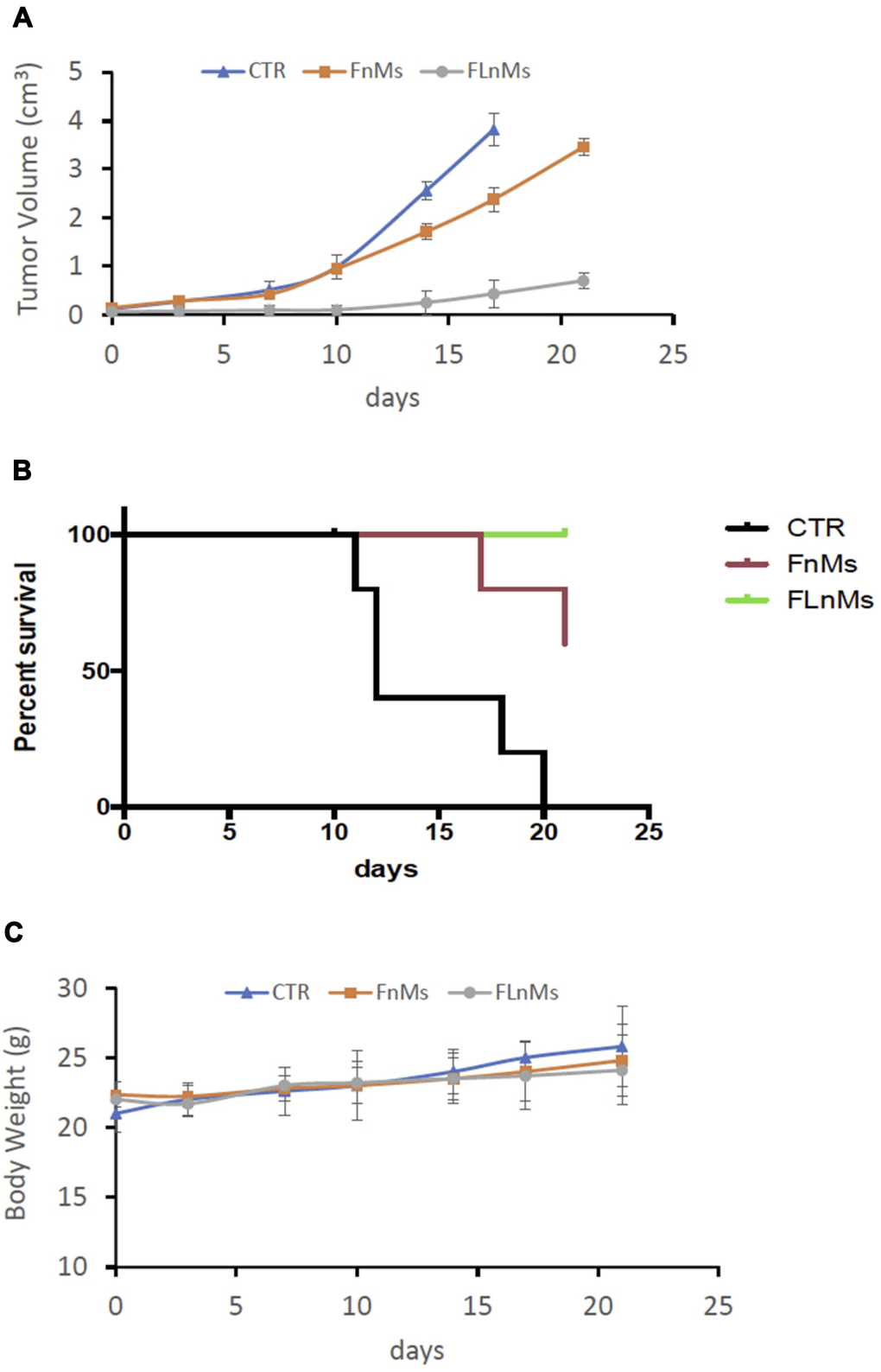

Figure 6 Efficacy of FLnMs and FnMs on BR6 flank xenografts. Cells were implanted subcutaneously in the flank of each mouse. Mice (n=4 per arm) were treated intravenously via tail vein injections with FLnMs (30 mg/kg fenretinide and 17 mg/kg Lenalidomide) or FnMs (30 mg/kg fenretinide) 3x/week for 3 weeks when tumors reached a volume of 0.1 cm^3. (**A**) Tumor growth inhibition. (**B**) Event-free survival curves of mice. (**C**) Body weight of mice during treatment. (mean ± SD, n = 4).

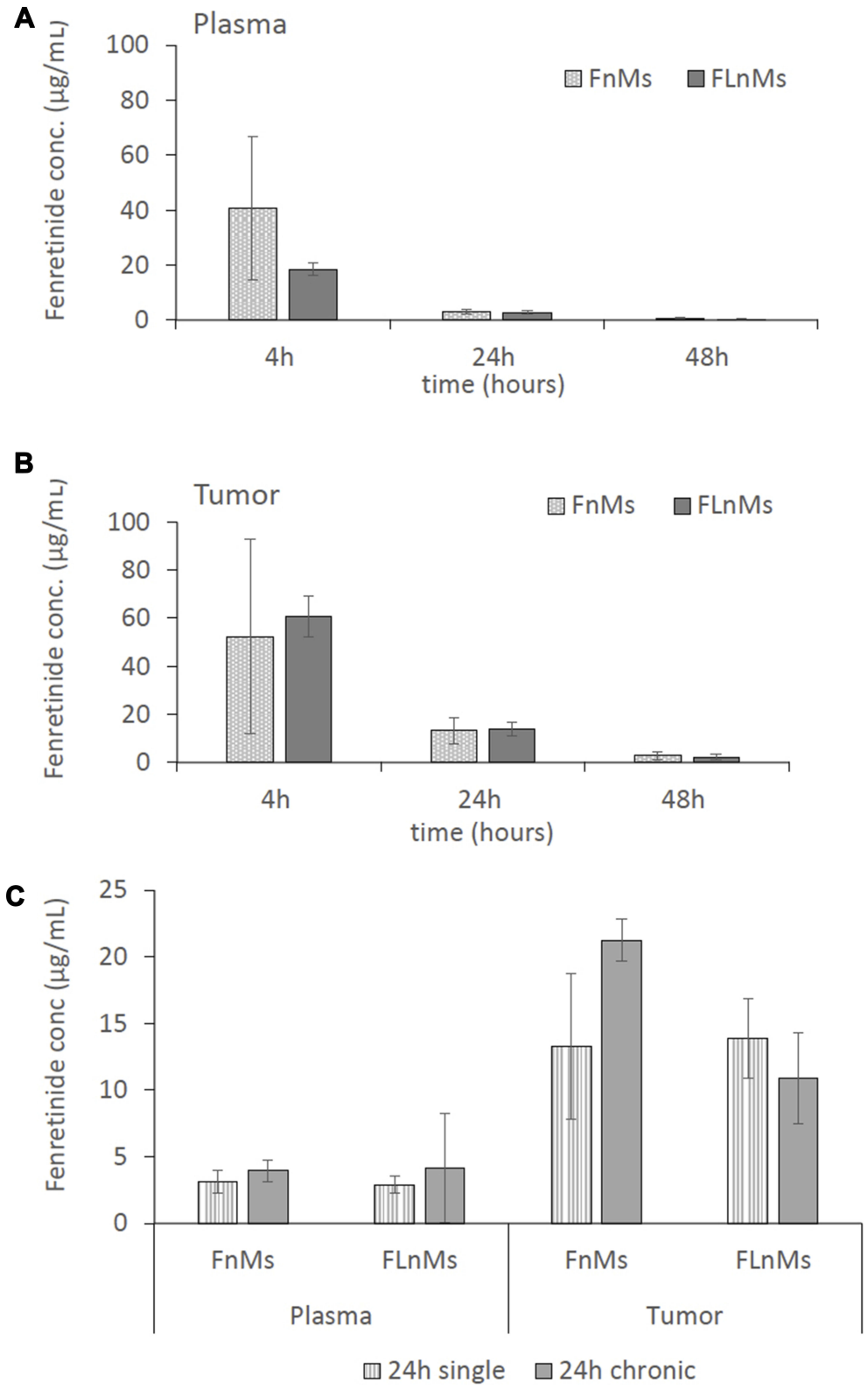

Figure 7 Plasma and tumor concentrations of fenretinide in mice treated with FLnMs and FnMs. Mice (n=3 per arm, per time point) were given a single dose of FLnMs (30 mg/kg fenretinide and 17 mg/kg Lenalidomide) or FnMs (30 mg/kg fenretinide) intravenously via tail vein. After 4, 24 and 48 h fenretinide levels were determined in plasma (**A**) and tumors (**B**). The mice treated with FLnMs (30 mg/kg fenretinide and 17 mg/kg Lenalidomide) or FnMs (30 mg/kg fenretinide) 3x/week for 3 weeks were sacrificed after 24 h from the last treatment and the concentrations of fenretinide were determined in plasma and tumors (**C**). (mean ± SD, n = 3).

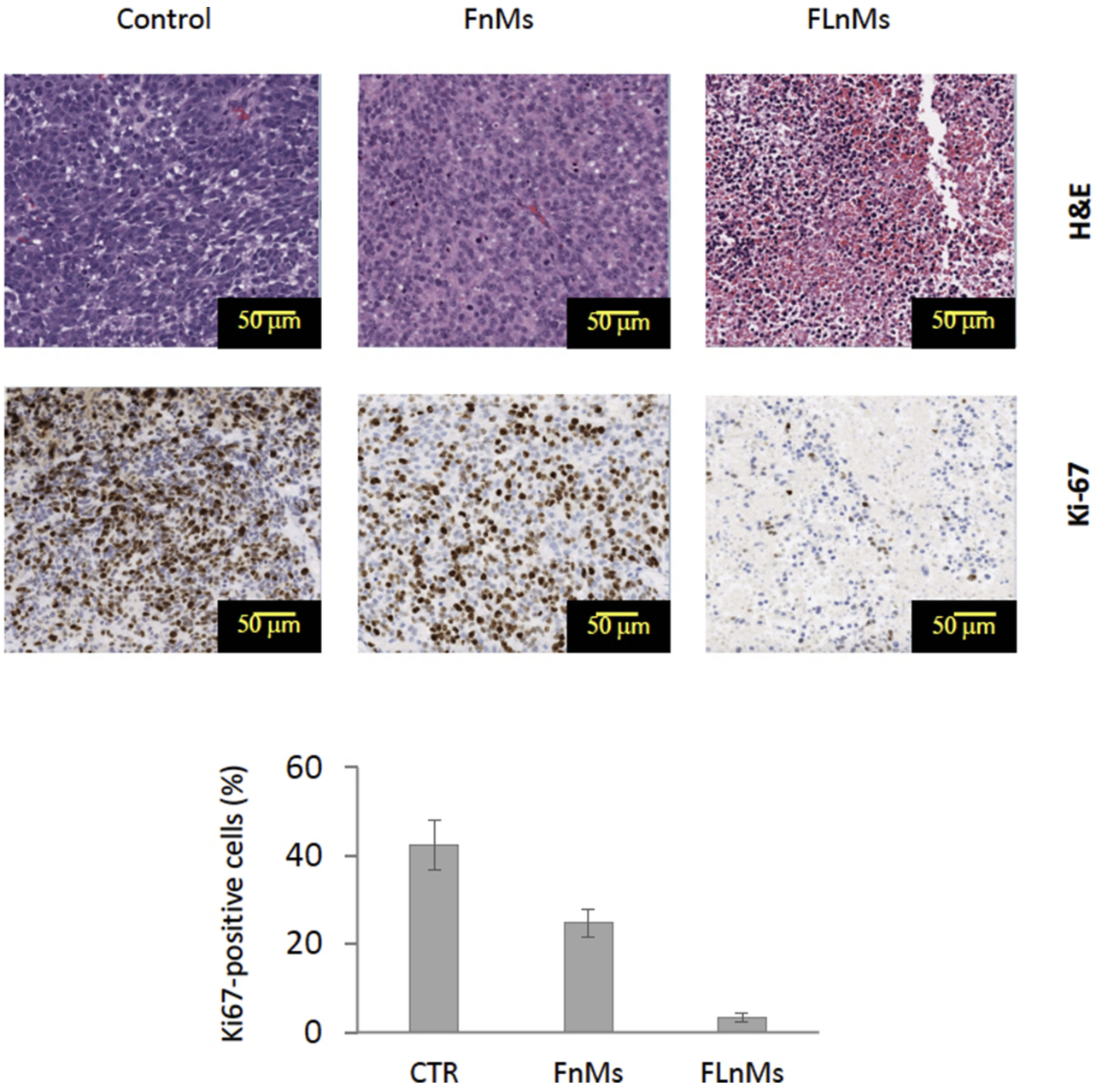

Figure 8 Histology of tumor samples. H&E staining of BR6 tumor xenografts: untreated tumors (Control) show packed undifferentiated cells, tumors treated with fenretinide (FnMs) are less compact and rich in neuropil, treatments with the fenretinide–lenalidomide combination (FLnMs) provide loose cells mostly differentiated with scarce active cells as demonstrated by the scant nuclear staining. Ki-67 staining show proliferation activity in untreated tumors (Control) with a proliferation index >30%, a decrease in proliferation in FnMs-treated tumors (proliferation index <25%) and a minimum proliferation activity in FLnMs-treated tumors (proliferation index <3%). (mean ± SD, n = 4).

In contrast, nanoparticle administration by oral route does not allow tumor accumulation by the EPR effect because the oral nanoparticles cannot cross the gastrointestinal mucosa in order to reach the circulation.[51] Their role is only to improve the drug solubilization in the gastrointestinal environment and thus enhance oral drug bioavailability. This may also increase drug concentration in tumors as a result of the increased drug-plasma concentration that affords biodistribution of increased drug amounts in the different body compartments, including the tumor site.[38]

However, repeated administration of oral nanoformulations is required to achieve high drug levels in tumors that would be comparable to those achieved by a single administration of a lower drug dose using intravenously injected nanoformulations.

Therefore, the high fenretinide concentrations obtained in NB tumors by FLnMs and FnMs accounted for the decrease in tumor growth observed with both nanoformulations compared to controls. The effect was evident after 10 days treatment (Figure 6A). The antitumor activity of FLnMs was higher than FnMs. Indeed, the tumor size after 21 days of treatment in mice receiving the combination was about sevenfold smaller than those receiving fenretinide alone, and the survival was 100% for the combination compared to only 70% for the single drug (Figure 6B). Chronic administration provided fenretinide concentrations in tumors that were higher for FnMs than for FLnMs (Figure 7C). Nevertheless, the antitumor activity was much greater for the fenretinide–lenalidomide combination compared to the nanomicelles with fenretinide alone. The antiangiogenic effect of lenalidomide is likely to account for the improved activity of the combination vs fenretinide alone, as lenalidomide did not show any cytotoxicity on the tumor cells in vitro.

It has been reported that the antiangiogenic activity of lenalidomide in tumors is mainly dependent on inhibition of Akt-1 phosphorylation in endothelial cells induced by VEGF.[42] This produces inhibitory effects on endothelial cell survival, association of adhesion junction protein complexes, migration and vessel formation.[43] As a result, lenalidomide not only represses the formation of new capillary tubes but also decreases the extension of the established capillary bed in tumors by inhibition of the endothelial cell survival.

Therefore, the antiangiogenic effect of lenalidomide may play a double role on the efficacy of the combination treatment by nanomicelles: 1) it reduces the supply of nutrients and oxygen to the tumor, and 2) it also decreases the surface of the tumor capillary endothelium available to nanomicelle extravasation. This causes a lowered nanomicelle extravasation, as demonstrated by the decreased concentration of fenretinide in tumors after chronic administration of FLnMs with respect to FnMs.

However, in spite of the decreased fenretinide concentration in tumors, FLnM administration provided superior antitumor activity compared to FnM administration. Probably the antiangiogenic effect of lenalidomide counterbalanced the decreased fenretinide concentration in tumors. Therefore, the induction of tumor starvation, due to the reduced supply of nutrients and oxygen, added to the cytotoxic activity of fenretinide, provided an overall superior antitumor effect than was achieved using single fenretinide treatment.

In this study, we used an athymic nude mice model that allowed us to evaluate the antiangiogenic effect of lenalidomide on FLnM activity. Further work is in progress with immunocompetent mouse models to evaluate the contribution of the immunomodulating effect of lenalidomide, reported in the NB microenvironment,[44] on the overall antitumor activity of the fenretinide–lenalidomide combination in FLnM nanomicelles.

Conclusion

In this study, we demonstrated that the combination of fenretinide with lenalidomide, administered by a novel nanomicellar formulation (FLnMs), provided a strong antitumor effect in an NB xenograft model. The nanomicelles had high encapsulation efficiency, mean sizes in the optimal range for tumor extravasation after intravenous administration, and the ability to provide high drug concentration in tumors. The nanomicelles containing the fenretinide–lenalidomide combination elicited an antitumor effect that was much higher than the nanomicelles containing fenretinide alone (FnMs), in spite of the absence of apparent cytotoxicity of lenalidomide on NB cells in vitro. This was attributed to the established antiangiogenic effect of lenalidomide that, together with the cytotoxic activity of fenretinide on the tumor cells, produced an improved overall antitumor effect. Therefore, the use of the fenretinide–lenalidomide combination in FLnMs represents a novel therapeutic approach to treat high-risk tumors, where repeated administration of low-toxicity agents is required over protracted time-periods to completely eradicate all residual tumor cells and avoid disease relapse. Drug accumulation at the tumor site by nanoencapsulation is the main requisite for a successful long-term therapy, as it guarantees high concentration levels of the active agents in the tumor environment, with minimal distribution to other organs and tissues throughout the body. Although FLnMs were tested in a model of NBs in this study, this novel therapeutic agent would be expected to be effective in many other solid tumors as well.

Disclosure

The authors report no conflicts of interest in this work.

References

1. Uemura S, Ishida T, Thwin KKM, et al. Dynamics of minimal residual disease in neuroblastoma patients. *Front Oncol*. 2019;4(9):455. doi:10.3389/fonc.2019.00455
2. Applebaum MA, Vaksman Z, Lee SM, et al. Neuroblastoma survivors are at increased risk for second malignancies: a report from the international neuroblastoma risk group project. *Eur J Cancer*. 2017;72:177–185. doi:10.1016/j.ejca.2016.11.022

3. Hobbie WL, Moshang Yang EJ, Wu C, Liu Y, Lv J, Sup Shim J. Revisiting non-cancer drugs for cancer therapy. *Curr Top Med Chem*. 2016;16(19):2144–2155. doi:10.2174/1568026616666160216154441
4. Cheung BB. Combination therapies improve the anticancer activities of retinoids in neuroblastoma. *World J Clin Oncol*. 2015;6(6):212–215. doi:10.5306/wjco.v6.i6.212
5. Garaventa A, Luksch R, Lo Piccolo MS, et al. Phase I trial and pharmacokinetics of fenretinide in children with neuroblastoma. *Clin Cancer Res*. 2003;9(6):2032–2039.
6. Maurer BJ, Kang MH, Villablanca JG, et al. Phase I trial of fenretinide delivered orally in a novel organized lipid complex in patients with relapsed/refractory neuroblastoma: a report from the new approaches to neuroblastoma therapy (NANT) consortium. *Pediatr Blood Cancer*. 2013;60:1801–1808. doi:10.1002/pbc.v60.11
7. Moore MM, Stockler M, Lim R, Mok TS, Millward M, Boyer MJ. A Phase II study of fenretinide in patients with hormone refractory prostate cancer: a trial of the cancer therapeutics research group. *Cancer Chemother Pharmacol*. 2010;66(5):845–850. doi:10.1007/s00280-009-1228-x
8. Schneider BJ, Worden FP, Gadgeel SM, et al. Phase II trial of fenretinide (NSC 374551) in patients with recurrent small cell lung cancer. *Invest New Drugs*. 2009;27(6):571–578. doi:10.1007/s10637-009-9228-6
9. Veronesi U, Mariani L, Decensi A, et al. Fifteen-year results of a randomized Phase III trial of fenretinide to prevent second breast cancer. *Ann Oncol*. 2006;17(7):1065–1071. doi:10.1093/annonc/mdl047
10. Villablanca JG, London WB, Naranjo A, et al. Phase II study of oral capsular 4-hydroxyphenylretinamide (4-HPR/fenretinide) in pediatric patients with refractory or recurrent neuroblastoma: a report from the children's oncology group. *Clin Cancer Res*. 2011;17(21):6858–6866. doi:10.1158/1078-0432.CCR-11-0995
11. Reynolds CP, Frgala T, Tsao-Wei DD, et al. High plasma levels of fenretinide (4-HPR) were associated with improved outcome in a phase II study of recurrent ovarian cancer: a study by the california cancer consortium. *J Clin Oncol*. 2007;25:5555.
12. Puduvalli VK, Yung WK, Hess KR; North American Brain Tumor Consortium, et al. Phase II study of fenretinide (NSC 374551) in adults with recurrent malignant gliomas: a North American brain tumor consortium study. *J Clin Oncol*. 2004;22(21):4282–4289. doi:10.1200/JCO.2004.09.096
13. Vaishampayan U, Heilbrun LK, Parchment RE, et al. Phase II trial of fenretinide in advanced renal carcinoma. *Invest New Drugs*. 2005;23:179–185. doi:10.1007/s10637-005-5864-7
14. Oridate N, Suzuki S, Higuchi M, Mitchell MF, Hong WK, Lotan R. Involvement of reactive oxygen species in N-(4-hydroxyphenyl)retinamide-induced apoptosis in cervical carcinoma cells. *J Natl Cancer Inst*. 1997;89(16):1191–1198. doi:10.1093/jnci/89.16.1191
15. Rahmaniyan M, Curley RW Jr, Obeid LM, Hannun YA, Kraveka JM. Identification of dihydroceramide desaturase as a direct in vitro target for fenretinide. *J Biol Chem*. 2011;286(28):24754–24764. doi:10.1074/jbc.M111.250779
16. Wang H, Maurer BJ, Liu -Y-Y, et al. N-(4-hydroxyphenyl)retinamide increases dihydroceramide and synergizes with dimethylsphingosine to enhance cancer cell killing. *Mol Cancer Ther*. 2008;7(9):2967–2976. doi:10.1158/1535-7163.MCT-08-0549
17. Xie H, Zhu F, Huang Z, et al. Identification of mammalian target of rapamycin as a direct target of fenretinide both in vitro and in vivo. *Carcinogenesis*. 2012;33(9):1814–1821. doi:10.1093/carcin/bgs234
18. Maurer B, Metelitsa L, Seeger R, Cabot M, Reynolds C. Increased of ceramide and induction of mixed apoptosis/necrosis by N-(4-hydroxyphenyl)retinamide in neuroblastoma cell lines. *J Natl Cancer Inst*. 1999;91:1138–1146. doi:10.1093/jnci/91.13.1138
19. Bassani B, Bartolini D, Pagani A, et al. Fenretinide (4-HPR) targets Caspase-9, ERK 1/2 and the Wnt3a/beta-catenin pathway in medulloblastoma cells and medulloblastoma cell spheroids. *PLoS One*. 2016;11(7):e0154111. doi:10.1371/journal.pone.0154111
20. Fettig LM, McGinn O, Finlay-Schultz J, LaBarbera DV, Nordeen SK, Sartorius CA. Cross talk between progesterone receptors and retinoic acid receptors in regulation of cytokeratin 5-positive breast cancer cells. *Oncogene*. 2017;36:6074–6084. doi:10.1038/onc.2017.204
21. Mukherjee N, Reuland SN, Lu Y, et al. Combining a BCL2 inhibitor with the retinoid derivative fenretinide targets melanoma cells including melanoma initiating cells. *J Invest Dermatol*. 2015;135(3):842–850. doi:10.1038/jid.2014.464
22. Yan W, Du J, Du Y, et al. Fenretinide targets the side population in myeloma cell line NCI-H929 and potentiates the efficacy of antimyeloma with bortezomib and dexamethasone regimen. *Leuk Res*. 2016;51:32–40. doi:10.1016/j.leukres.2016.10.010
23. Villablanca JG, Krailo MD, Ames MM, Reid JM, Reaman GH, Reynolds CP. Phase I trial of oral fenretinide in children with high-risk solid tumors: a report from the Children's Oncology Group (CCG 09709). *J Clin Oncol*. 2006;24(21):3423–3430. doi:10.1200/JCO.2005.03.9271
24. Jasti BR, LoRusso PM, Parchment RE, Wozniak AJ, Flaherty LE, Shields AF. Phase I clinical trial of fenretinide (NSC374551) in advanced solid tumors. *Proc Am Soc Clin Oncol*. 2001;20:122a.
25. Cooper JP, Hwang K, Singh H, et al. Fenretinide metabolism in humans and mice: utilizing pharmacological modulation of its metabolic pathway to increase systemic exposure. *Br J Pharmacol*. 2011;163(6):1263–1275. doi:10.1111/j.1476-5381.2011.01310.x
26. Maurer BJ, Kalous O, Yesair DW, et al. Improved oral delivery of N-(4-hydroxyphenyl)retinamide with a novel LYM-X-SORB organized lipid complex. *Clin Cancer Res*. 2007;13(10):3079–3086. doi:10.1158/1078-0432.CCR-06-1889
27. Kummar S, Gutierrez ME, Maurer BJ, et al. Phase I trial of fenretinide lym-x-sorb oral powder in adults with solid tumors and lymphomas. *Anticancer Res*. 2011;31(3):961–966.
28. Mohrbacher AM, Yang AS, Groshen S, et al. Phase I study of fenretinide delivered intravenously in patients with relapsed or refractory hematologic malignancies: a california cancer consortium trial. *Clin Cancer Res*. 2017;23(16):4550–4555. doi:10.1158/1078-0432.CCR-17-0234
29. Cooper JP, Reynolds CP, Cho H, Kang MH. Clinical development of fenretinide as an antineoplastic drug: pharmacology perspectives. *Exp Biol Med (Maywood)*. 2017;242(11):1178–1184. doi:10.1177/1535370217706952
30. Orienti I, Zuccari G, Falconi M, Teti G, Illingworth NA, Veal GJ, Novel micelles based on amphiphilic branched PEG as carriers for fenretinide. *Nanomedicine*. 2012;6:880–890. doi:10.1016/j.nano.2011.10.008
31. Orienti I, Zuccari G, Carosio R, Montaldo PG. Improvement of aqueous solubility of fenretinide and other hydrophobic anti-tumor drugs by complexation with amphiphilic dextrins. *Drug Deliv*. 2009;16(7):389–398. doi:10.1080/10717540903101655
32. Orienti I, Zuccari G, Bergamante V, et al. Amphiphilic poly(vinyl alcohol) derivatives as complexing agents for fenretinide. *Biomacromolecules*. 2006;7(11):3157–3163. doi:10.1021/bm060482s
33. Pignatta S, Orienti I, Falconi M, et al. Albumin nanocapsules containing fenretinide: pre-clinical evaluation of cytotoxic activity in experimental models of human non-small cell lung cancer. *Nanomedicine*. 2015;11(2):263–273. doi:10.1016/j.nano.2014.10.004
34. Durante S, Orienti I, Teti G, et al. Anti-tumor activity of fenretinide complexed with human serum albumin in lung cancer xenograft mouse model. *Oncotarget*. 2014;5(13):4811–4820. doi:10.18632/oncotarget.v5i13
35. Falconi M, Focaroli S, Teti G, et al. Novel PLA microspheres with hydrophilic and bioadhesive surfaces for the controlled delivery of fenretinide. *J Microencapsul*. 2014;31(1):41–48. doi:10.3109/02652048.2013.805838
36. Di Paolo D, Pastorino F, Zuccari G, et al. Enhanced anti-tumor and anti-angiogenic efficacy of a novel liposomal fenretinide on human neuroblastoma. *J Control Release*. 2013;170(3):445–451. doi:10.1016/j.jconrel.2013.06.015

37. Orienti I, Francescangeli F, De Angelis ML, et al. A new bioavailable fenretinide formulation with antiproliferative, antimetabolic, and cytotoxic effects on solid tumors. *Cell Death Dis*. 2019;10(7):529. doi:10.1038/s41419-019-1775-y
38. Orienti I, Salvati V, Sette G, et al. A novel oral micellar fenretinide formulation with enhanced bioavailability and antitumour activity against multiple tumours from cancer stem cells. *J Exp Clin Cancer Res*. 2019;38(1):373. doi:10.1186/s13046-019-1383-9
39. Dredge K, Marriott JB, Macdonald CD, et al. Novel thalidomide analogues display anti-angiogenic activity independently of immunomodulatory effects. *Br J Cancer*. 2002;87:1166–1172. doi:10.1038/sj.bjc.6600607
40. Kotla V, Goel S, Nischal S, et al. Mechanism of action of lenalidomide in hematological malignancies. *J Hematol Oncol*. 2009;2:36. doi:10.1186/1756-8722-2-36
41. Buesche G, Dieck S, Giagounidis A, et al. Antiangiogenic in vivo effect of lenalidomide (CC-5013) in myelodysplastic syndrome with del (5q) chromosome abnormality and its relation to the course of disease [abstract]. *Blood*. 2005;106(suppl):. doi:10.1182/blood-2004-04-1622
42. Dredge K, Horsfall R, Robinson SP, et al. Orally administered lenalidomide (CC-5013) is anti-angiogenic in vivo and inhibits endothelial cell migration and Akt phosphorylation in vitro. *Microvasc Res*. 2005;69(1–2):56–63. doi:10.1016/j.mvr.2005.01.002
43. Lu L, Payvandi F, Wu L, et al. The anti-cancer drug lenalidomide inhibits angiogenesis and metastasis via multiple inhibitory effects on endothelial cell function in normoxic and hypoxic conditions. *Microvasc Res*. 2009;77(2):78–86. doi:10.1016/j.mvr.2008.08.003
44. Xu Y, Sun J, Sheard MA, et al. Lenalidomide overcomes suppression of human natural killer cell anti-tumor functions by neuroblastoma microenvironment-associated IL-6 and TGFβ1. *Cancer Immunol Immunother*. 2013;62(10):1637–1648. doi:10.1007/s00262-013-1466-y
45. Roy Choudhury S, Karmakar S, Banik NL, Ray SK. Targeting angiogenesis for controlling neuroblastoma. *J Oncol*. 2012;15:2012.
46. Pereira S, Egbu R, Jannati G, Al-Jamal WT. Docetaxel-loaded liposomes: the effect of lipid composition and purification on drug encapsulation and in vitro toxicity. *Int J Pharm*. 2016;514(1):150–159. doi:10.1016/j.ijpharm.2016.06.057
47. Mennucci B, Tomasi J. Continuum solvation models: a new approach to the problem of solute's charge distribution and cavity boundaries. *J Chem Phys*. 1997;106:5151–5155. doi:10.1063/1.473558
48. Nguyen F, Alferiev I, Guan P, et al. Enhanced intratumoral delivery of SN38 as a tocopherol oxyacetate prodrug using nanoparticles in a neuroblastoma xenograft model. *Clin Cancer Res*. 2018;24(11):2585–2593. doi:10.1158/1078-0432.CCR-17-3811
49. Torchilin VP. Passive and active drug targeting: drug delivery to tumors as an example. *Handb Exp Pharmacol*. 2010;197:3–53.
50. Golombek SK, May JN, Theek B, et al. Tumor targeting via EPR: strategies to enhance patient responses. *Adv Drug Deliv Rev*. 2018;130:17–38. doi:10.1016/j.addr.2018.07.007
51. Date AA, Hanes J, Ensign LM. Nanoparticles for oral delivery: design, evaluation and state-of-the-art. *J Control Release*. 2016;28(240):504–526. doi:10.1016/j.jconrel.2016.06.016